https://doi.org/10.5194/wes-2026-169
Preprint. Discussion started: 20 November 2026
© Author(s) 2026. CC BY 4.0 License.

eawe european academy of wind energy
Open Access WIND ENERGY SCIENCE DISCUSSIONS

Matching Aerodynamic Forces with Flaps in the Blade Element Momentum Theory

Arthur Scolari Fagundes[coer]
[coer]Centre for Ocean Energy Research, Maynooth University, Ireland.
Correspondence: Arthur Scolari Fagundes (arthurscolari@gmail.com)

Abstract. The contribution of this paper is a method based on least-squares optimization and blade element momentum theory for determining a flap deflection that minimizes the differences between target and actual aerodynamic loads prioritized by weighting parameters. Numerical examples illustrate the selection of targets and weighting parameters and show that prioritized loads are accurately tracked. The method is applied to linearize the relation between loads and blade pitch deviations and to reduce periodic loads induced by nonuniform wind. The resulting flap trajectory is compared with a harmonic parameterization commonly adopted in the literature. Finally, formulations with both affine and nonlinear lift and drag coefficients are evaluated.

1 Introduction

Considering factors such as a variable rotor speed and non-uniform wind speed profile, each blade of a wind turbine is susceptible to varying aerodynamic loads over a single rotation. As the blades rotate, these varying loads become periodic in nature (Jelavic et al., 2008). Moreover, the varying loads have a positive relation with rotor size, which has continued to grow with the development of increasingly large offshore wind turbines.

The individual pitch control (IPC) was applied for load reduction in Bossanyi (2003). A second goal of the IPC is tower stabilization, to the benefit of offshore platforms. Regarding the first objective, however, the IPC has a caveat: the same pitch variations $\Delta\beta$ used to compensate one component of the aerodynamic loads may induce pulsations in another. Regarding the second goal, another issue, considering that linearity is a common premise of control design methods, is that the relation between the control signals in u and the average moments that result from the aerodynamic loads may be nonlinear.

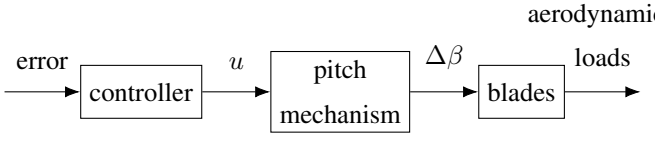


Figure 1. IPC diagram

As indicated by Fig. 1, the relation between the control signal u and the aerodynamic loads can be modified by the pitch mechanism, e.g. by a swashplate that modifies the sinusoidal relation between blade pitch and azimuth that characterizes Paul Cornu's mechanism (Leishman and Johnson, 2009), or, alternatively, by blades equipped with active control surfaces Barlas and van Kuik (2010), such as active trailing edge flaps.

https://doi.org/10.5194/wes-2026-169
Preprint. Discussion started: 20 November 2026
© Author(s) 2026. CC BY 4.0 License.



eawe european academy of wind energy
Open Access WIND ENERGY SCIENCE DISCUSSIONS

Experimental flaps have been used in Gamberini et al. (2024) for model validation, and in McWilliam et al. (2018) for energy production maximization. Gomez Gonzalez et al. (2021) shows with a full-scale wind turbine that the flaps can be used to manipulate aerodynamic loads. A review is presented in Madsen (2024). A numerical model governed by Navier-Stokes equations spatially filtered by Large-Eddy Simulation is used by Huang et al. (2019) to show that the flaps can be used to disturb tip vortices.

Related to the present work, Millott and Friedmann (1994) considered active control flaps for vibration reduction using aerodynamic coefficients that depend on flap actuation. That work also compared flaps and IPC through a cost function that penalizes vibration magnitudes. Although the reported results indicate improved performance with flaps for that particular criterion, Friedmann and Millott (1995) concluded that their main advantage does not lie in vibration reduction *per se*, but in substantially lower actuation-power requirements.

This paper starts with an extension to the blade element theory where the lift and drag coefficients are defined as nonlinear or affine functions of the flap deflection. The use of a coefficient associated to the presence of a flap or another type of control surface is seen in Millott and Friedmann (1994) for vibration reduction using active control flaps (ACF). On a side note, the figure 57 of that reference compares the values obtained with flaps or IPC for a cost function (eq. 9.1 therein) that penalizes vibration magnitudes. Whereas the previous reference suggests a better performance of the flaps, Friedmann and Millott (1995) conclude that the advantage of the flaps is not in the vibration reduction *per se*, but in the power requirements, that are an order of magnitude smaller.

The strategy proposed here differs from that of Millott and Friedmann (1994) in the definition of the optimization objective. Rather than directly penalizing vibration magnitudes, the quadratic cost function introduced in this paper penalizes deviations of selected aerodynamic loads from prescribed targets. To formulate this problem, blade element momentum theory is extended by allowing the lift and drag coefficients to depend affinely or nonlinearly on the flap deflection. The resulting formulation makes explicit the compromise among different aerodynamic-load components through weighting parameters and provides a means of determining a flap deflection $\hat{\delta}$ that minimizes the corresponding weighted load-tracking error.

2 Blade element theory with lift and drag coefficients depending on flap deflection

2.1 The wind turbine

Fig. 2 illustrates the rotor and the i-th blade element moving downwards. In the rotor, θ and $\Omega = \dot{\theta}$ are the azimuth and rotor angular speed, β is the pitch of one blade and r is the rotor radius.

In the i-th blade element, where $i \in \{1, ..., n\}$, a_i and b_i are the axial and tangential induction factors, $V_{(\infty)i}$ is the upstream wind speed, $V_{(\text{rel})i}$ is the relative wind speed, r_i and dr_i are respectively the blade element radius and width, α_i is the angle of attack, $\beta + \gamma_i$ is the blade pitch angle plus local twist, and $\phi_i = \beta + \gamma_i + \alpha_i$ is the inflow angle. Finally, $\delta_i \in [0, 1]$ is the flap element deflection.

https://doi.org/10.5194/wes-2026-169
Preprint. Discussion started: 20 November 2026
© Author(s) 2026. CC BY 4.0 License.

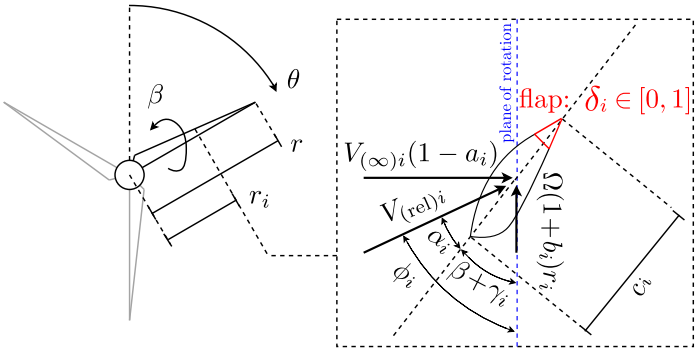


Figure 2. Wind turbine rotor and blade element.

In the velocity triangle, the opposite side is $V_{(\infty)i}(1-a_i)$ and the adjacent side is $\Omega r(1+b_i)$, which leads to the inflow angle and relative wind speed expressions:

$$\phi_i = \tan^{-1}\left(\left(V_{(\infty)i}(1-a_i)\right)/\left(\Omega(1+b_i)r_i\right)\right) \tag{1}$$

$$V_{(\mathrm{rel})i} = \sqrt{(V_{(\infty)i}(1-a_i))^2 + (\Omega(1+b_i)r_i)^2} \tag{2}$$

Considering ρ the air density, let

$$q_i = \tfrac{1}{2}\rho V_{(\mathrm{rel})i}^2 c_i dr_i \tag{3}$$

be the load multiplier at blade element i. The lift and drag acting on a blade element are $F_{(\mathrm{L})i} = q_i C_{(\mathrm{L})i}$ and $F_{(\mathrm{D})i} = q_i C_{(\mathrm{D})i}$, where $C_{(\mathrm{L})i} = C_{(\mathrm{L})i}(\alpha_i, \delta_i)$ and $C_{(\mathrm{D})i} = C_{(\mathrm{D})i}(\alpha_i, \delta_i)$ are the lift and drag coefficients as functions of the angle of attack

$$\alpha_i = \phi_i - (\beta + \gamma_i) \tag{4}$$

and the flap element deflection δ_i.

The projections of $F_{(\mathrm{L})i}$ and $F_{(\mathrm{D})i}$ onto the plane of rotation result in the normal and tangential forces $F_{(\mathrm{N})i} = q_i C_{(\mathrm{N})i}$ and $F_{(\mathrm{T})i} = q_i C_{(\mathrm{T})i}$, where the normal and tangential coefficients are related to the lift and drag coefficients $C_{(\mathrm{N})i} = C_{(\mathrm{L})i}\cos(\phi_i) + C_{(\mathrm{D})i}\sin(\phi_i)$ and $C_{(\mathrm{T})i} = C_{(\mathrm{L})i}\sin(\phi_i) - C_{(\mathrm{D})i}\cos(\phi_i)$. The contributions of a blade element i for the thrust, torque and root bending moment are respectively

$$T_i = \left(F_{(\mathrm{L})i}\cos(\phi_i) + F_{(\mathrm{D})i}\sin(\phi_i)\right) = F_{(\mathrm{N})i},$$

$$Q_i = \left(F_{(\mathrm{L})i}\sin(\phi_i) - F_{(\mathrm{D})i}\cos(\phi_i)\right) r_i = F_{(\mathrm{T})i} r_i,$$

and

$$\tau_{(\mathrm{N})i} = F_{(\mathrm{N})i} r_i.$$

The annulus swept by blade element i has a mass flow $m_i = 2\pi r_i \rho V_{(\infty)i}(1-a_i)dr_i$. The thrust at blade element i is

$$T_{(\mathrm{BEM})i} = m_i 2a_i V_{(\infty)i} = 4\pi r_i a_i \rho V_{(\infty)i}^2 (1-a_i) dr_i,$$

https://doi.org/10.5194/wes-2026-169
Preprint. Discussion started: 20 November 2026
© Author(s) 2026. CC BY 4.0 License.



eawe european academy of wind energy
Open Access WIND ENERGY SCIENCE DISCUSSIONS

and the torque is

$$Q_{(\mathrm{BEM})i} = m_i 2b_i\Omega r_i^2 = 4\pi\rho V_{(\infty)i}(1-a_i)b_i\Omega r_i^3 dr_i.$$

Proposition 1 (Branlard (2017)) If $T_i = T_{(\mathrm{BEM})i}$, then the axial induction factor satisfies the implicit equation

$$a_i(\alpha_i,\delta_i) = \left(1+4\sin^2\phi_i/\left(\sigma_i C_{(\mathrm{N})i}(\alpha_i,\delta_i)\right)\right)^{-1} \tag{5}$$

where $\sigma_i = \frac{c_i}{2\pi r_i}$ is the solidity factor. Similarly, if $Q_i = Q_{(\mathrm{BEM})i}$, then the tangential induction factor satisfies

$$b_i(\alpha_i,\delta_i) = \left(4\sin\phi_i\cos\phi_i/\left(\sigma_i C_{(\mathrm{T})i}(\alpha_i,\delta_i)\right)-1\right)^{-1}. \tag{6}$$

Proof. From Eq. (1) one has $\Omega(1+b_i)r_i = (1-a_i)V_{(\infty)i}/\tan\phi_i$. Substituting in Eq. (2) gives $V_{(\mathrm{rel})i} = (1-a_i)V_{(\infty)i}/\sin\phi_i$, which applied to $T_i = F_{(\mathrm{N})i} = q_i C_{(\mathrm{N})i}$ results in $T_i = \frac{1}{2}\rho\big((1-a_i)V_{(\infty)i}/\sin\phi_i\big)^2 c_i dr_i C_{(\mathrm{N})i}$. From the equality $T_i = T_{(\mathrm{BEM})i}$, one obtains Eq. (5) after cancelling $\rho V_{(\infty)i}^2(1-a_i)dr_i$ on both sides and rearranging the equation. Likewise, using $(1-a_i)V_{(\infty)i} = (1+b_i)\Omega r_i\tan\phi_i$ gives $V_{(\mathrm{rel})i} = (1+b_i)\Omega r_i/\cos\phi_i$, which applied to $Q_i = F_{(\mathrm{T})i}r_i = q_i C_{(\mathrm{T})i}r_i$ results in $Q_i = \frac{1}{2}\rho\big((1-a_i)V_{(\infty)i}/\sin\phi_i\big)\big((1+b_i)\Omega r_i/\cos\phi_i\big)c_i dr_i C_{(\mathrm{T})i}r_i$. From the equality $Q_i = Q_{(\mathrm{BEM})i}$, one obtains Eq. (6). ■

2.2 Matching aerodynamic loads with flap deflection

An updated flap element deflection is denoted $\hat{\delta}_i$. This section is started with the following assumption:

Assumption 1 After the instantaneous update of a flap element deflection, denoted $\delta_i \leftarrow \hat{\delta}_i$, the rotor speed, wind speed and blade pitch angle remain the same.

Since the induction factors a_i and b_i depend on δ_i, the assumption above does not include α_i, q_i and ϕ_i as constants, i.e., the velocity triangle changes with a flap update. To calculate the updated velocity triangle angles, consider, from Eq. (1), Eq. (5) and Eq. (6), the inflow angle in terms of $a_i(\hat{\alpha}_i,\hat{\delta}_i)$ and $b_i(\hat{\alpha}_i,\hat{\delta}_i)$:

$$\hat{\phi}_i \triangleq \tan^{-1}\left(\frac{V_{(\infty)i}\big(1-a_i(\hat{\alpha}_i,\hat{\delta}_i)\big)}{\Omega r_i\big(1+b_i(\hat{\alpha}_i,\hat{\delta}_i)\big)}\right) \tag{7}$$

where, recalling from Eq. (4) that $\phi_i = \beta+\gamma_i+\alpha_i$,

$$\hat{\alpha}_i \triangleq \hat{\phi}_i - (\beta+\gamma_i). \tag{8}$$

Replacing $a_i(\hat{\alpha}_i,\hat{\delta}_i)$ and $b_i(\hat{\alpha}_i,\hat{\delta}_i)$ in the relative wind speed eq. Eq. (2) and then in Eq. (3) yields the load multiplier after a flap deflection update:

$$\hat{q}_i = \tfrac{1}{2}\rho\Big(\big(V_{(\infty)i}\big(1-a_i(\hat{\alpha}_i,\hat{\delta}_i)\big)\big)^2 + \big(\Omega r_i\big(1+b_i(\hat{\alpha}_i,\hat{\delta}_i)\big)\big)^2\Big)c_i dr_i, \tag{9}$$

where $a_i(\hat{\alpha}_i,\hat{\delta}_i)$ and $b_i(\hat{\alpha}_i,\hat{\delta}_i)$ are given by Proposition 1.

Since $\hat{\alpha}_i$ is obtained from $\hat{\delta}_i$ in Eq. (8), the notation $C_{(\mathrm{L})i}(\hat{\alpha}_i,\hat{\delta}_i) \triangleq C_{(\mathrm{L})i}(\hat{\delta}_i)$, $C_{(\mathrm{D})i}(\hat{\alpha}_i,\hat{\delta}_i) \triangleq C_{(\mathrm{D})i}(\hat{\delta}_i)$, $C_{(\mathrm{N})i}(\hat{\alpha}_i,\hat{\delta}_i) \triangleq C_{(\mathrm{N})i}(\hat{\delta}_i)$ and $C_{(\mathrm{T})i}(\hat{\alpha}_i,\hat{\delta}_i) \triangleq C_{(\mathrm{T})i}(\hat{\delta}_i)$ is adopted henceforth. The same applies to the blade element thrust and torque, whose updates are denoted by $T_i(\hat{\delta}_i) = \hat{q}_i C_{(\mathrm{N})i}(\hat{\delta}_i)$ and $Q_i(\hat{\delta}_i) = \hat{q}_i C_{(\mathrm{T})i}(\hat{\delta}_i)r_i$.

https://doi.org/10.5194/wes-2026-169
Preprint. Discussion started: 20 November 2026
© Author(s) 2026. CC BY 4.0 License.



eawe european academy of wind energy
Open Access WIND ENERGY SCIENCE DISCUSSIONS

There is no guarantee of the existence of $\hat{\delta}_i$ such that the updated aerodynamic loads simultaneously match arbitrarily chosen targets $T_i^\star$, $Q_i^\star$, $\tau_{(\mathrm{N})i}^\star$ and $F_{(\mathrm{T})i}^\star$, that is, such that $T_i(\hat{\delta}_i) = T_i^\star$, $Q_i(\hat{\delta}_i) = Q_i^\star$, $\tau_{(\mathrm{N})i}(\hat{\delta}_i) = \tau_{(\mathrm{N})i}^\star$ and $F_{(\mathrm{T})i}(\hat{\delta}_i) = F_{(\mathrm{T})i}^\star$ are satisfied. Therefore, the errors $\Delta T_i \triangleq T_i^\star - T_i(\hat{\delta}_i)$, $\Delta Q_i \triangleq Q_i^\star - Q_i(\hat{\delta}_i)$, and so on are defined as part of the following cost function:

$$\tilde{J} \triangleq \zeta_2 \sum_{i=1}^{n} \left(\zeta_1 \left(\frac{\Delta T_i}{\max T^\star} \right)^2 + (1-\zeta_1) \left(\frac{\Delta Q_i}{\max Q^\star} \right)^2 \right) + (1-\zeta_2) \sum_{i=1}^{n} \left(\zeta_1 \left(\frac{\Delta \tau_{(\mathrm{N})i}}{\max \tau_{(\mathrm{N})}^\star} \right)^2 + (1-\zeta_1) \left(\frac{\Delta F_{(\mathrm{T})i}}{\max F_{(\mathrm{T})}^\star} \right)^2 \right)$$

where $\zeta_1, \zeta_2 \in [0,1]$ are weighting parameters, and $\max T^\star$, $\max Q^\star$, $\max \tau_{(\mathrm{N})}^\star$ and $\max F_{(\mathrm{T})}^\star$ are the maximum values in the sets $\{T_1^\star, ..., T_n^\star\}$, $\{Q_1^\star, ..., Q_n^\star\}$, $\{\tau_{(\mathrm{N})1}^\star, ..., \tau_{(\mathrm{N})n}^\star\}$ and $\{F_{(\mathrm{T})1}^\star, ..., F_{(\mathrm{T})\mathrm{n}}^\star\}$, respectively. The errors are divided by their respective targets to be normalized and dimensionless, and then squared to be nonnegative. Finally, the squared terms are summed—summing before squaring could otherwise yield a null cost even when individual errors are nonzero.

Flaps typically do not span the entire length of a blade and certainly do not operate by individual elements. Therefore, consider $\mathcal{F}$ the set with the flap elements, and $\hat{\delta}$ the flap deflection, that is, $\hat{\delta}_i = \hat{\delta}$ for $i \in \mathcal{F}$, and, contrarily, the neutral deflection is $\hat{\delta}_i = \delta_\mathrm{x}$ for $i \notin \mathcal{F}$. One has that

$$\Delta T_i = \begin{cases} T_i^\star - T_i(\hat{\delta}) & \text{if } i \in \mathcal{F} \\ T_i^\star - T_i(\delta_\mathrm{x}) & \text{if } i \notin \mathcal{F} \end{cases}, \quad \Delta Q_i = \begin{cases} Q_i^\star - Q_i(\hat{\delta}) & \text{if } i \in \mathcal{F} \\ Q_i^\star - Q_i(\delta_\mathrm{x}) & \text{if } i \notin \mathcal{F} \end{cases}, \quad \Delta \tau_{(\mathrm{N})i} = \begin{cases} \tau_{(\mathrm{N})i}^\star - \tau_{(\mathrm{N})i}(\hat{\delta}) & \text{if } i \in \mathcal{F} \\ \tau_{(\mathrm{N})i}^\star - \tau_{(\mathrm{N})i}(\delta_\mathrm{x}) & \text{if } i \notin \mathcal{F} \end{cases}, \quad \Delta F_{(\mathrm{T})i} = \begin{cases} F_{(\mathrm{T})i}^\star - F_{(\mathrm{T})i}(\hat{\delta}) & \text{if } i \in \mathcal{F} \\ F_{(\mathrm{T})i}^\star - F_{(\mathrm{T})i}(\delta_\mathrm{x}) & \text{if } i \notin \mathcal{F} \end{cases}$$

For compactness, let the loads be generically denoted by Y, and the weighting parameters by h:

$$\big(Y_{(j,k)i}, h_{(j,k)}\big) \triangleq \begin{cases} \big(T_i \quad, \zeta_2\zeta_1\big), & \text{if } (j,k) = (0,0), \\ \big(Q_i \quad, \zeta_2(1-\zeta_1)\big), & \text{if } (j,k) = (1,1), \\ \big(\tau_{(\mathrm{N})i}, (1-\zeta_2)\zeta_1\big), & \text{if } (j,k) = (0,1), \\ \big(F_{(\mathrm{T})i}, (1-\zeta_2)(1-\zeta_1)\big), & \text{if } (j,k) = (1,0), \end{cases} \tag{10}$$

The generic error is thus $\Delta Y_{(j,k)i}(\hat{\delta}) \triangleq Y_{(j,k)i}^\star - Y_{(j,k)i}(\hat{\delta})$.

Consider $S_\mathcal{F}(\hat{\delta})$ the portion of $\tilde{J}$ such that $i \in \mathcal{F}$, and $S_{\not\mathcal{F}}$ the portion of $\tilde{J}$ such that $i \notin \mathcal{F}$, that is:

$$S_\mathcal{F}(\hat{\delta}) \triangleq \sum_{i\in\mathcal{F}} \sum_{j=0}^{1} \sum_{k=0}^{1} h_{(j,k)} \left(\frac{\Delta Y_{(j,k)i}(\hat{\delta})}{\max Y_{(j,k)}^\star} \right)^2,$$

$$S_{\not\mathcal{F}} \triangleq \sum_{i\notin\mathcal{F}} \sum_{j=0}^{1} \sum_{k=0}^{1} h_{(j,k)} \left(\frac{Y_{(j,k)i}^\star - Y_{(j,k)i}(\delta_\mathrm{x})}{\max Y_{(j,k)}^\star} \right)^2.$$

Since $S_{\not\mathcal{F}}$ is constant in $\hat{\delta}$, the argument that minimizes $\tilde{J} = S_\mathcal{F}(\hat{\delta}) + S_{\not\mathcal{F}}$ and $J \triangleq S_\mathcal{F}(\hat{\delta})$ is the same. Differentiating the cost function, one has

$$\frac{dJ}{d\hat{\delta}} = -2 \sum_{i\in\mathcal{F}} \sum_{j=0}^{1} \sum_{k=0}^{1} h_{(j,k)} \frac{\Delta Y_{(j,k)i}(\hat{\delta})}{\left(\max Y_{(j,k)}^\star\right)^2} \frac{dY_{(j,k)i}(\hat{\delta})}{d\hat{\delta}} \tag{11}$$

https://doi.org/10.5194/wes-2026-169
Preprint. Discussion started: 20 November 2026
© Author(s) 2026. CC BY 4.0 License.



eawe european academy of wind energy
Open Access WIND ENERGY SCIENCE DISCUSSIONS

The next sections shows how to compute $\hat{\delta}$ with least squares optimization.

2.2.1 Nonlinear coefficients

For compactness, consider

$$C_{(\mathrm{N})i} \triangleq C_{(0)i} \text{ and } C_{(\mathrm{T})i} \triangleq C_{(1)i} \tag{12}$$

Theorem The minimizer of $J(\hat{\delta})$ is

$$\hat{\delta} = \frac{-E(\hat{\delta}) \pm \sqrt{E^2(\hat{\delta}) - 4D(\hat{\delta})F(\hat{\delta})}}{2F(\hat{\delta})}, \tag{13}$$

provided that $F \neq 0$, $\frac{d^2J}{d\hat{\delta}^2} > 0$ and $E^2 - 4DF \geq 0$.

Where $D(\hat{\delta}) = \sum_{i\in\mathcal{F}}\sum_{j=0}^{1}\sum_{k=0}^{1} h_{(j,k)}\, D_{(j,k)i}(\hat{\delta})$,

and $E(\hat{\delta}) = \sum_{i\in\mathcal{F}}\sum_{j=0}^{1}\sum_{k=0}^{1} h_{(j,k)}\, E_{(j,k)i}(\hat{\delta})$,

and $F(\hat{\delta}) = \sum_{i\in\mathcal{F}}\sum_{j=0}^{1}\sum_{k=0}^{1} h_{(j,k)}\, F_{(j,k)i}(\hat{\delta})$,

and $D_{(j,k)i}(\hat{\delta}) = \left(\max Y^{\star}_{(j,k)}\right)^{-2}\left(Y^{\star}_{(j,k)i} r_i^k \hat{q}_i \frac{dC_{(j)i}(\hat{\delta})}{d\hat{\delta}} + Y^{\star}_{(j,k)i} r_i^k \frac{d\hat{q}_i}{d\hat{\delta}}\left(C_{(j)i}(\hat{\delta}) - \hat{\delta}\frac{dC_{(j)i}(\hat{\delta})}{d\hat{\delta}}\right) - \ldots \right.$

$\left. \ldots r_i^{2k}\hat{q}_i^2 \frac{dC_{(j)i}(\hat{\delta})}{d\hat{\delta}}\left(C_{(j)i}(\hat{\delta}) - \hat{\delta}\frac{dC_{(j)i}(\hat{\delta})}{d\hat{\delta}}\right) - r_i^{2k}\hat{q}_i\frac{d\hat{q}_i}{d\hat{\delta}}\left(C_{(j)i}(\hat{\delta}) - \hat{\delta}\frac{dC_{(j)i}(\hat{\delta})}{d\hat{\delta}}\right)^2 \right)$,

and $E_{(j,k)i}(\hat{\delta}) = \left(\max Y^{\star}_{(j,k)}\right)^{-2}\left(Y^{\star}_{(j,k)i} r_i^k \frac{d\hat{q}_i}{d\hat{\delta}} - r_i^{2k}\hat{q}_i^2 \frac{dC_{(j)i}(\hat{\delta})}{d\hat{\delta}} - 2r_i^{2k}\hat{q}_i\frac{d\hat{q}_i}{d\hat{\delta}}\left(C_{(j)i}(\hat{\delta}) - \hat{\delta}\frac{dC_{(j)i}(\hat{\delta})}{d\hat{\delta}}\right)\right)\frac{dC_{(j)i}(\hat{\delta})}{d\hat{\delta}}$,

and $F_{(j,k)i}(\hat{\delta}) = \left(\max Y^{\star}_{(j,k)}\right)^{-2}\left(- r_i^{2k}\hat{q}_i\frac{d\hat{q}_i}{d\hat{\delta}}\left(\frac{dC_{(j)i}(\hat{\delta})}{d\hat{\delta}}\right)^2\right)$.

Proof. From the compact notation for generic loads and coefficients in (10) and (12), one has

$$Y_{(j,k)i}(\hat{\delta}) = r_i^k \hat{q}_i C_{(j)i}(\hat{\delta}),$$

and

$$\frac{dY_{(j,k)i}(\hat{\delta})}{d\hat{\delta}} = r_i^k\left(\hat{q}_i\frac{dC_{(j)i}(\hat{\delta})}{d\hat{\delta}} + C_{(j)i}(\hat{\delta})\frac{d\hat{q}_i}{d\hat{\delta}}\right).$$

The coefficient can be written as

$$C_{(j)i}(\hat{\delta}) = C_{(j)i}(\hat{\delta}) - \hat{\delta}\frac{dC_{(j)i}(\hat{\delta})}{d\hat{\delta}} + \hat{\delta}\frac{dC_{(j)i}(\hat{\delta})}{d\hat{\delta}}.$$

https://doi.org/10.5194/wes-2026-169
Preprint. Discussion started: 20 November 2026
© Author(s) 2026. CC BY 4.0 License.



eawe european academy of wind energy
Open Access WIND ENERGY SCIENCE DISCUSSIONS

Therefore,

$$Y_{(j,k)i}(\hat{\delta}) = r_i^k \hat{q}_i \left(C_{(j)i}(\hat{\delta}) - \hat{\delta}\frac{dC_{(j)i}(\hat{\delta})}{d\hat{\delta}} + \hat{\delta}\frac{dC_{(j)i}(\hat{\delta})}{d\hat{\delta}} \right)$$

and

$$\frac{dY_{(j,k)i}(\hat{\delta})}{d\hat{\delta}} = r_i^k \left(\hat{q}_i \frac{dC_{(j)i}(\hat{\delta})}{d\hat{\delta}} + \frac{d\hat{q}_i}{d\hat{\delta}} \left(C_{(j)i}(\hat{\delta}) - \hat{\delta}\frac{dC_{(j)i}(\hat{\delta})}{d\hat{\delta}} + \hat{\delta}\frac{dC_{(j)i}(\hat{\delta})}{d\hat{\delta}} \right) \right).$$

Consequently,

$$\Delta Y_{(j,k)i}(\hat{\delta}) = Y^{\star}_{(j,k)i} - r_i^k \hat{q}_i \left(C_{(j)i}(\hat{\delta}) - \hat{\delta}\frac{dC_{(j)i}(\hat{\delta})}{d\hat{\delta}} + \hat{\delta}\frac{dC_{(j)i}(\hat{\delta})}{d\hat{\delta}} \right).$$

Substituting these expressions in Eq. (11), multiplying the terms and grouping them according to the powers of $\hat{\delta}$ gives

$$\begin{aligned} \frac{dJ}{d\hat{\delta}} &= -2 \sum_{i \in \mathcal{F}} \sum_{j=0}^{1} \sum_{k=0}^{1} h_{(j,k)} \left(D_{(j,k)i}(\hat{\delta}) + E_{(j,k)i}(\hat{\delta})\hat{\delta} + F_{(j,k)i}(\hat{\delta})\hat{\delta}^2 \right) \\ &= -2\left(D(\hat{\delta}) + E(\hat{\delta})\hat{\delta} + F(\hat{\delta})\hat{\delta}^2 \right). \end{aligned} \tag{14}$$

Setting $dJ/d\hat{\delta} = 0$ yields the expression for a stationary point $\hat{\delta} = (-E \pm \sqrt{E^2 - 4DF})/(2F)$. The root with positive second derivative and no imaginary part is then selected with $\frac{d^2J}{d\hat{\delta}^2} > 0$ and $E^2 - 4DF \geq 0$, respectively. ■

Notice that the value of $\hat{\delta}$ is implicit in Eq. (13). Analogously to how a_i and b_i are computed in classic blade element momentum algorithms from the implicit equations of Proposition 1, $\hat{\delta}$ can be iteratively computed from Eq. (13): an initial guess is applied into its right-hand side, yielding a guess result on the left-hand side, which becomes the new guess in the next iteration, until the guess and its result are approximately the same. The initial guess is the neutral flap deflection δ_x.

Recalling that the hat symbol $\hat{}$ denotes a variable after the flap update, the inflow angle $\hat{\phi}_i$, angle of attack $\hat{\alpha}_i$ and load multiplier $\hat{q}_i$ from Eq. (7), Eq. (8) and Eq. (9) are also implicit. For this reason, in Algorithm A3 they have their hat removed, because only the last iteration is the true value after the flap update.

Finally, the terms $\frac{d\hat{q}_i}{d\hat{\delta}}$ and $\frac{dC_{(j)i}(\hat{\delta})}{d\hat{\delta}}$ are also replaced by their derivatives evaluated at the current guess δ, which are read as $\frac{q_i - q_{(\mathrm{prev})i}}{\delta_i - \delta_{(\mathrm{prev})i}}$ and $\frac{C_{(\mathrm{j})i} - C_{(\mathrm{j})(\mathrm{prev})i}}{\delta_i - \delta_{(\mathrm{prev})i}}$.

2.2.2 affine coefficients

For a given angle of attack, the lift and drag coefficients are assumed affine with respect to the flap deflection:

$$C_{(\mathrm{L})i}(\hat{\delta}) \triangleq C_{(\mathrm{L})i}(0) + S_{(\mathrm{L})i}\hat{\delta},\ C_{(\mathrm{D})i}(\hat{\delta}) \triangleq C_{(\mathrm{D})i}(0) + S_{(\mathrm{D})i}\hat{\delta}.$$

The normal and tangential coefficients are consequently described by

$$C_{(\mathrm{N})i}(\hat{\delta}) = C_{(\mathrm{N})i}(0) + S_{(\mathrm{N})i}\hat{\delta},\ C_{(\mathrm{T})i}(\hat{\delta}) = C_{(\mathrm{T})i}(0) + S_{(\mathrm{T})i}\hat{\delta}. \tag{15}$$

https://doi.org/10.5194/wes-2026-169
Preprint. Discussion started: 20 November 2026
© Author(s) 2026. CC BY 4.0 License.



eawe european academy of wind energy
Open Access WIND ENERGY SCIENCE DISCUSSIONS

where
$$C_{(\mathrm{N})i}(0) = C_{(\mathrm{L})i}(0)\cos\hat{\phi}_i + C_{(\mathrm{D})i}(0)\sin\hat{\phi}_i \tag{16}$$
and
$$C_{(\mathrm{T})i}(0) = C_{(\mathrm{L})i}(0)\sin\hat{\phi}_i - C_{(\mathrm{D})i}(0)\cos\hat{\phi}_i \tag{17}$$
and
$$S_{(\mathrm{N})i} = S_{(\mathrm{L})i}\cos\hat{\phi}_i + S_{(\mathrm{D})i}\sin\hat{\phi}_i \tag{18}$$
and
$$S_{(\mathrm{T})i} = S_{(\mathrm{L})i}\sin\hat{\phi}_i - S_{(\mathrm{D})i}\cos\hat{\phi}_i. \tag{19}$$

The derivatives with respect to $\hat{\phi}_i$ follow

$$\frac{dC_{(\mathrm{N})i}}{d\hat{\delta}} = S_{(\mathrm{N})i} + \left(\frac{dC_{(\mathrm{N})i}(0)}{d\hat{\phi}_i} + \hat{\delta}\frac{dS_{(\mathrm{N})i}}{d\hat{\phi}_i}\right)\frac{d\hat{\phi}_i}{d\hat{\delta}}, \tag{20}$$

$$\frac{dC_{(\mathrm{T})i}}{d\hat{\delta}} = S_{(\mathrm{T})i} + \left(\frac{dC_{(\mathrm{T})i}(0)}{d\hat{\phi}_i} + \hat{\delta}\frac{dS_{(\mathrm{T})i}}{d\hat{\phi}_i}\right)\frac{d\hat{\phi}_i}{d\hat{\delta}}. \tag{21}$$

In the next corollary, consider $S_{(\mathrm{N})i} \triangleq S_{(0)i}$ and $S_{(\mathrm{T})i} \triangleq S_{(1)i}$

Corollary Provided that

$$|S_{(\mathrm{j})i}| \gg \left|\left(\frac{dC_{(\mathrm{j})i}(0)}{d\hat{\phi}_i} + \hat{\delta}\frac{dS_{(\mathrm{j})i}}{d\hat{\phi}_i}\right)\frac{d\hat{\phi}_i}{d\hat{\delta}}\right| \text{ for } \begin{matrix} j \in \{0,1\} \\ i \in \{1,\ldots,n\} \end{matrix}$$

and $F \neq 0$, $\frac{d^2J}{d\hat{\delta}^2} > 0$ and $E^2 - 4DF \geq 0$, the approximate minimizer of $J(\hat{\delta})$ is given by Eq. (13) parameterized as follows:

$$D_{(j,k)i}(\hat{\delta}) = \left(\max Y^{\star}_{(j,k)}\right)^{-2}\left(Y^{\star}_{(j,k)i}\, r_i^k \hat{q}_i S_{(j)i} + Y^{\star}_{(j,k)i} r_i^k \frac{d\hat{q}_i}{d\hat{\delta}} C_{(j)i}(0) - r_i^{2k}\hat{q}_i^2 S_{(j)i} C_{(j)i}(0) - r_i^{2k}\hat{q}_i \frac{d\hat{q}_i}{d\hat{\delta}} C_{(j)i}(0)^2\right),$$

and $$E_{(j,k)i}(\hat{\delta}) = \left(\max Y^{\star}_{(j,k)}\right)^{-2}\left(Y^{\star}_{(j,k)i} r_i^k \frac{d\hat{q}_i}{d\hat{\delta}} - r_i^{2k}\hat{q}_i^2 S_{(j)i} - 2r_i^{2k}\hat{q}_i \frac{d\hat{q}_i}{d\hat{\delta}} C_{(j)i}(0)\right) S_{(j)i},$$

and $$F_{(j,k)i}(\hat{\delta}) = \left(\max Y^{\star}_{(j,k)}\right)^{-2}\left(-r_i^{2k}\hat{q}_i \frac{d\hat{q}_i}{d\hat{\delta}} S^2_{(j)i}\right).$$

Proof. In Eq. (11), make the following substitutions:

$$Y_{(j,k)i}(\hat{\delta}) = r_i^k \hat{q}_i C_{(j)i}(\hat{\delta}), \quad \frac{dY_{(j,k)i}(\hat{\delta})}{d\hat{\delta}} = r_i^k\left(\hat{q}_i \frac{dC_{(j)i}(\hat{\delta})}{d\hat{\delta}} + C_{(j)i}(\hat{\delta})\frac{d\hat{q}_i}{d\hat{\delta}}\right)$$

In the resulting expression, replace $C_{(j)i}(\hat{\delta})$ according to Eq. (15)–(19), and replace $\frac{dC_{(j)i}(\hat{\delta})}{d\hat{\delta}}$ according to Eq. (20) and Eq. (21). Under the assumption of the corollary, $\frac{dC_{(\mathrm{j})i}}{d\hat{\delta}} \approx S_{(\mathrm{j})i}$. Grouping the terms in powers of $\hat{\delta}$ yield Eq. (14), with the coefficients D, E, and F given above. ■

Notice that the assumption of the corollary is not easily verified *a priori*. It is verified *a posteriori* through the accuracy of the numerical results.

https://doi.org/10.5194/wes-2026-169
Preprint. Discussion started: 20 November 2026
© Author(s) 2026. CC BY 4.0 License.



eawe european academy of wind energy
Open Access WIND ENERGY SCIENCE DISCUSSIONS

2.3 Choosing targets and weighting parameters

To define the targets $Y^{\star}_{(j,k)i}$, consider their sum given as

$$Y^{\star}_{(j,k)} \triangleq \sum_{i=1}^{n} Y^{\star}_{(j,k)i}.$$

The loads that must be exerted by the flaps to match $Y^{\star}_{(j,k)}$ are

$$Y^{\star}_{(j,k)\mathcal{F}} \triangleq Y^{\star}_{(j,k)} - Y^{\star}_{(j,k)\not{\mathcal{F}}},$$

where $Y^{\star}_{(j,k)\not{\mathcal{F}}}$ is the total load produced by flapless blade elements. $Y^{\star}_{(j,k)}$ is distributed among the blade elements $i \in \mathcal{F}$ as

$$Y^{\star}_{(j,k)i} = w_{(j,k)i}\, Y^{\star}_{(j,k)\mathcal{F}}\, \text{sign}\left(Y^{\star}_{(j,k)\mathcal{F}}\right)$$

with weights

$$w_{(j,k)i} = \frac{Y_{(j,k)i}}{\left|\sum_{\ell\in\mathcal{F}} Y_{(j,k)\ell}\right|}, \qquad i \in \mathcal{F},\ \ j,k \in \{0,1\}.$$

The choice of $Y^{\star}_{(j,k)}$ and weighting parameters ζ_1 and ζ_2 depends on the user's goal. In the next section, the numerical examples will illustrate some choices.

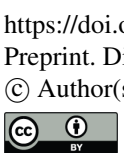
3 Numerical results

Three examples are exposed. In the first, the relation between one component of the aerodynamic loads and deviations in the blade pitch ($\Delta\beta$) is linearized by the use of flaps. The advantage of a linear torque is that, since the sum of symmetrical phasors is zero, the contributions of each blade cancel out and pulsation is eliminated. The advantage of a linear root bending moment is on the responsivity - the relation between the control signals applied to the pitch and yaw axes of the fixed frame and the resulting moments around the same axes is also linear. The first example, in which ζ_1 and ζ_2 are in $\{0,1\}^2$, will show that the prioritized targets can be precisely tracked. The second example is to find ζ_1 and ζ_2 such that vibration producing loads are minimized. The resulting flap trajectory is then compared with another trajectory restricted to a prescribed set of harmonic basis functions. The third example illustrates the case of nonlinear coefficients, comparing the resulting flap deflections and aerodynamic loads with those obtained with affine coefficients.

3.1 Example 1 - linearization of aerodynamic loads and pitch deviations

What has been developed so far allows the computation of $Y_{(j,k)i}(\beta)$ (load in terms of blade pitch) for each blade. The relation between blade pitch β and azimuth θ by the MBC transformation follows, so $Y_{(j,k)i}(\theta)$ can be obtained. Consider β_1, β_2 and β_3 the blade pitches of a 3 blade rotor, and τ_y and τ_z respectively the pitch (or tilt) and yaw moments, and the blade rotation angles $\theta_3 = \theta_2 + 2\pi/3 = \theta_1 + 4\pi/3$d, as seen in Fig. 3.

https://doi.org/10.5194/wes-2026-169
Preprint. Discussion started: 20 November 2026
© Author(s) 2026. CC BY 4.0 License.



eawe european academy of wind energy
Open Access WIND ENERGY SCIENCE DISCUSSIONS

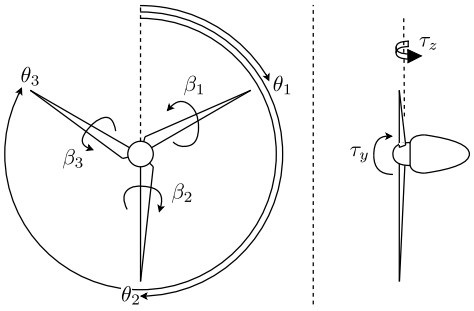


Figure 3. Azimuth, individual blade pitches (left) and hub moments (right).

Consider $\theta_1 \triangleq \theta$ the azimuth. For $i = 1,2,3$, the pitch equations are expressed as $\beta_i = \beta_c + \Delta\beta_i$, where β_c is the collective angle and the individual deviations are expressed according to the MBC transformation:

$$\Delta\beta_1 = u_y \sin(\theta + \pi/2) \qquad + u_z \sin(\theta)$$
$$\Delta\beta_2 = u_y \sin(\theta + \pi/2 + 2\pi/3) + u_z \sin(\theta + 2\pi/3)$$
$$\Delta\beta_3 = u_y \sin(\theta + \pi/2 + 4\pi/3) + u_z \sin(\theta + 4\pi/3)$$

where u_y and u_z are the individual flap signals for pitch and yaw moments, respectively. Consider $\tau_{(\mathrm{N})}$ the total root bending moment of the first blade, expressed as a function of the azimuth by $\tau_{(\mathrm{N})}(\theta) = \sum_{i=1}^{n} \tau_{(\mathrm{N})i}(\theta) = \sum_{i=1}^{n} r_i T_i(\theta)$. The resulting average moments $\bar{\tau}_y$ and $\bar{\tau}_z$ in the pitch and yaw axes of the hub are

$$\bar{\tau}_y = \frac{3}{2\pi} \int_0^{2\pi} \tau_{(\mathrm{N})}(\theta) \cos(\theta) d\theta, \; \bar{\tau}_z = \frac{3}{2\pi} \int_0^{2\pi} \tau_{(\mathrm{N})}(\theta) \sin(\theta) d\theta.$$

Considering $C_{(\mathrm{L})\mathrm{i},\mathrm{IEA15MW}}$ and $C_{(\mathrm{D})\mathrm{i},\mathrm{IEA15MW}}$ the original airfoil coefficients of the IEA 15MW (flapless) wind turbine for $i \in [1,2,...,n]$ and $n = 50$ blade elements, assume that two flaps are installed, one from element 5 to 22 and another from element 28 to 45. Thus, for $i \in \mathcal{F} = [5,22] \cup [28,45]$. The coefficients are

$$C_{(\mathrm{L})i}(\hat{\delta}) = \left(\frac{1}{2} + \frac{3}{2}\hat{\delta}\right) C_{(\mathrm{L}),\mathrm{IEA15MW}},$$
$$C_{(\mathrm{D})i}(\hat{\delta}) = \left(\frac{1}{2} + \frac{3}{2}\hat{\delta}\right) C_{(\mathrm{D}),\mathrm{IEA15MW}}.$$

The neutral flap deflection is therefore $\delta_{\mathrm{x}} = 1/3$, for which the original IEA 15 MW aerodynamic coefficients are recovered. The sensitivities of the normal and tangential coefficients used in the corollary are consequently

$$S_{(\mathrm{N})i} = \frac{3}{2}\left(C_{(\mathrm{L})i,\mathrm{IEA15MW}} \cos\hat{\phi}_i + C_{(\mathrm{D})i,\mathrm{IEA15MW}} \sin\hat{\phi}_i\right),$$

and

$$S_{(\mathrm{T})i} = \frac{3}{2}\left(C_{(\mathrm{L})i,\mathrm{IEA15MW}} \sin\hat{\phi}_i - C_{(\mathrm{D})i,\mathrm{IEA15MW}} \cos\hat{\phi}_i\right).$$

https://doi.org/10.5194/wes-2026-169
Preprint. Discussion started: 20 November 2026
© Author(s) 2026. CC BY 4.0 License.

The turbine is in steady state, with constant rotor speed ($\Omega = 4$ rpm) and uniform wind speed ($V = 18$ m/s) with a typical air density ($\rho = 1.225$ kg/m^3). The grid of blade pitches, $X_\beta = \{\beta_{(\text{grid})j_\beta} : j_\beta = 1, \cdots, 61\}$, is delimited by $\beta_{(\text{grid})1} = 0$ and $\beta_{(\text{grid})61} = 30$ degrees, in steps of 0.5.

In this scenario, the blue curves in Fig. 4 are the aerodynamic loads as a function of blade pitch in just one of the blades of the flapless IEA 15MW wind turbine. The orange lines are the targets, crossing intermediate points of the corresponding flapless curves. Visibly, the targets are chosen to linearize the relation between a selected aerodynamic load and deviations in the blade pitch.

In the first four plots, the weighting parameters are $\zeta_1 = 1$ and $\zeta_2 = 0$. In this case, the root bending moment $\tau_{(N)}$ is precisely tracked. For $\zeta_1 = 0$ and $\zeta_2 = 1$ the next four plots show the torque Q prioritized and tracked. The last two plots show the corresponding flap deflection $\hat{\delta}$ in each case.

The individual flap signals are then chosen as $u_y = 10$ and $u_z = 0$ degrees so β stays within the the limits of the grid X_β. and the resulting torque obtained with $\zeta_1 = 0$ in the presence and absence of flaps is plotted in Fig. 5. Then, with $\zeta_1 = 1$ and combinations of $u_y, u_z \in [1, 5]$ in a 25x25 grid, the root bending moment response with and without the flaps compensation is compared in Fig. 6. The flat surfaces show a linear responsivity.

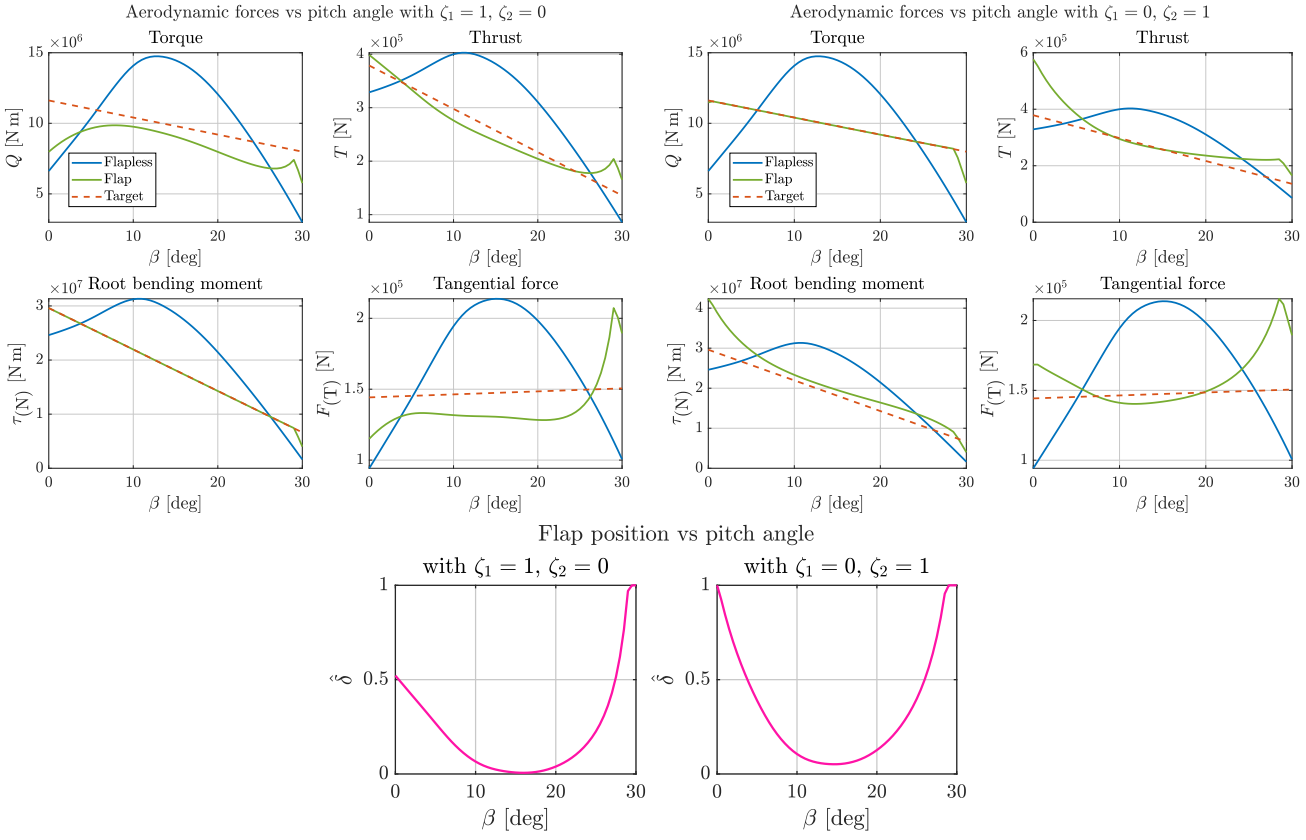


Figure 4. Aerodynamic loads and flap deflection vs pitch angle of one blade

https://doi.org/10.5194/wes-2026-169
Preprint. Discussion started: 20 November 2026
© Author(s) 2026. CC BY 4.0 License.



WIND ENERGY SCIENCE DISCUSSIONS

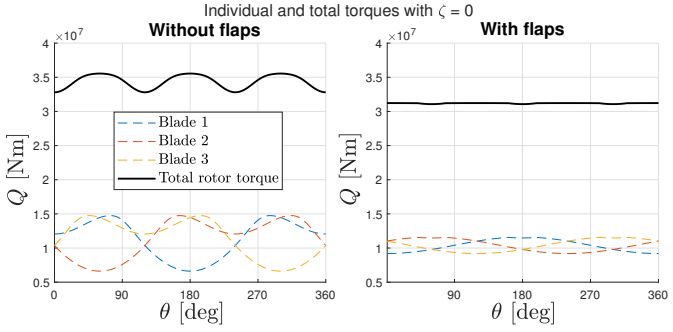


Figure 5. Torque pulsation for $\zeta_1 = 0$, $\zeta_2 = 1$.

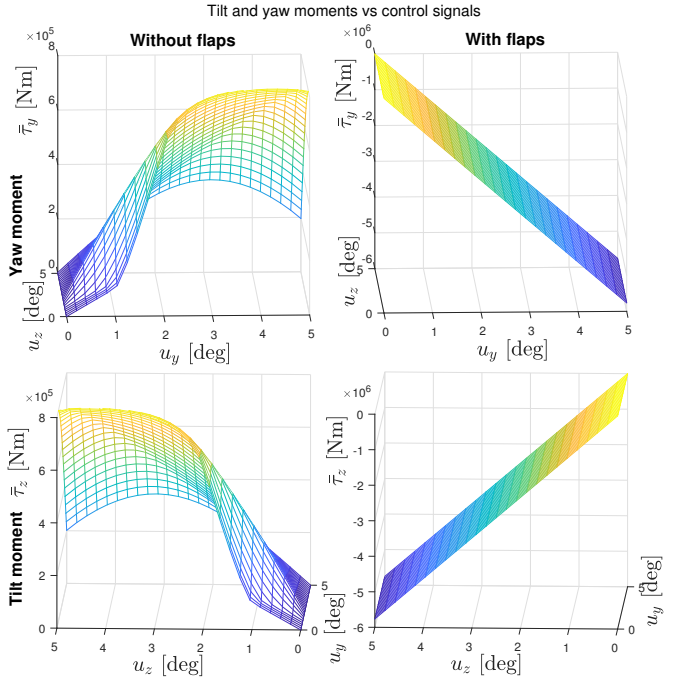


Figure 6. Root bending moments response compensation

3.2 Example 2 - reduction of wind induced load pulsations

In this example, the first goal is to determine the combination of ζ_1 and ζ_2 that minimizes wind induced load pulsations. The second goal is to investigate the effect of restricting the flap trajectory to a finite set of harmonic functions. Such a parameterization is commonly adopted in the literature and can be written as

$$\delta(\theta) = \delta_c + \sum_{m=m_{\min}}^{m_{\max}} \left(\delta_{\cos,m}\cos(m\theta) + \delta_{\sin,m}\sin(m\theta)\right). \tag{22}$$

The parameters of the previous example are contemplated again, except by the wind speed profile and blade pitch. Now, the pulsations are caused by the wind, not the flap movement. A constant collective pitch of $\beta_c = 15°$ is adopted, with no individual

https://doi.org/10.5194/wes-2026-169
Preprint. Discussion started: 20 November 2026
© Author(s) 2026. CC BY 4.0 License.



eawe european academy of wind energy
Open Access WIND ENERGY SCIENCE DISCUSSIONS

pitch variations, and the wind-speed profile is assumed to be described by a power law combined with tower shadow. Thus, the inflow velocity is given by

$$V_{(\infty)}(\theta, r) = V_{\text{hub}} \left(\frac{H_{\text{hub}} + r\cos\theta}{H_{\text{hub}}} \right)^{\nu} \left(\frac{K_t}{r} \right)^2 \cos^2(\theta - \pi) \mathbf{1}_{|\theta-\pi| \leq \pi/8}$$

where V_{hub} is the inflow speed at hub height H_{hub}, z is the height from the ground, and ν is the shear exponent, K_t is a constant associated to the tower shadow and $\mathbf{1}_{|\theta-\pi/2| \leq \pi/8}$ is an indicator function delimiting the tower shadow to the azimuth sector $\pi/2 \pm \pi/8$.

Recalling τ_y and τ_z from Fig. 3 and denoting τ_x the moment around the x axis, and F_x, F_y and F_z the translation loads in the same axes, their expressions are given as follows:

$$F_x(\theta) = T(\theta_1) + T(\theta_2) + T(\theta_3),$$

$$F_y(\theta) = -F_{(\text{T})}(\theta_1)\cos\theta_1 - F_{(\text{T})}(\theta_2)\cos\theta_2 - F_{(\text{T})}(\theta_3)\cos\theta_3,$$
$$F_z(\theta) = -F_{(\text{T})}(\theta_1)\sin\theta_1 - F_{(\text{T})}(\theta_2)\sin\theta_2 - F_{(\text{T})}(\theta_3)\sin\theta_3,$$

$$\tau_x(\theta) = Q(\theta_1) + Q(\theta_2) + Q(\theta_3),$$
$$\tau_y(\theta) = \tau_{(\text{N})}(\theta_1)\cos\theta_1 + \tau_{(\text{N})}(\theta_2)\cos\theta_2 + \tau_{(\text{N})}(\theta_3)\cos\theta_3,$$
$$\tau_z(\theta) = \tau_{(\text{N})}(\theta_1)\sin\theta_1 + \tau_{(\text{N})}(\theta_2)\sin\theta_2 + \tau_{(\text{N})}(\theta_3)\sin\theta_3.$$

Using the notation $F^{(m)}$ for the m-th harmonic of the load F, the harmonic-load index for the three forces and three moments is defined as in Viswamurthy and Ganguli (2004):

$$J_v^{(m)} = \sqrt{\left(\frac{F_x^{(m)}}{F_{\text{ref}}}\right)^2 + \left(\frac{F_y^{(m)}}{F_{\text{ref}}}\right)^2 + \left(\frac{F_z^{(m)}}{F_{\text{ref}}}\right)^2} + \sqrt{\left(\frac{\tau_x^{(m)}}{\tau_{\text{ref}}}\right)^2 + \left(\frac{\tau_y^{(m)}}{\tau_{\text{ref}}}\right)^2 + \left(\frac{\tau_z^{(m)}}{\tau_{\text{ref}}}\right)^2}, \tag{23}$$

where $F_{\text{ref}} = 1$ N, and $\tau_{\text{ref}} = 1$ N/m. Since the rotor has 3 blades and each one is subject to loads that vary once per revolution, the predominant harmonics are multiples of 3. Therefore, we will consider in particular only $J_v^{(3)}$, $J_v^{(6)}$, $J_v^{(9)}$ and $J_v^{(12)}$. Additionally, the harmonic-load index is defined as

$$J_v = \sqrt{J_v^{(3)} + J_v^{(6)} + J_v^{(9)} + J_v^{(12)}}. \tag{24}$$

First, the value of J_v obtained with flaps is evaluated at $\zeta_1, \zeta_2 \in [0, 1]$. As seen in the next figure, in this case the edge $\zeta_1 = 1$, $\zeta_2 = 0$ resulted in the least cost.

https://doi.org/10.5194/wes-2026-169
Preprint. Discussion started: 20 November 2026
© Author(s) 2026. CC BY 4.0 License.



eawe european academy of wind energy
Open Access WIND ENERGY SCIENCE DISCUSSIONS

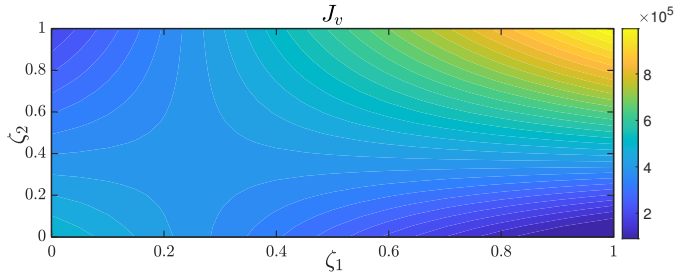


Figure 7. Harmonic-load index (24) for different combinations of ζ_1 and ζ_2.

In Fig. 8, a comparison is conducted by fitting Eq. (22) to the flap deflection obtained with $\zeta_1 = 1$ and $\zeta_2 = 0$, the minimum in Fig. 7. As a baseline, the index without flaps is

$$J_v = 468590.$$

The index with the flap activation given by $\hat{\delta} = \frac{-E \pm \sqrt{E^2 - 4DF}}{2F}$ is

$$J_v = 100481,$$

while the approximation of Eq. (22) with $m_{\min} = 1$ and $m_{\max} = 5$ results in

$$J_v = 179538.$$

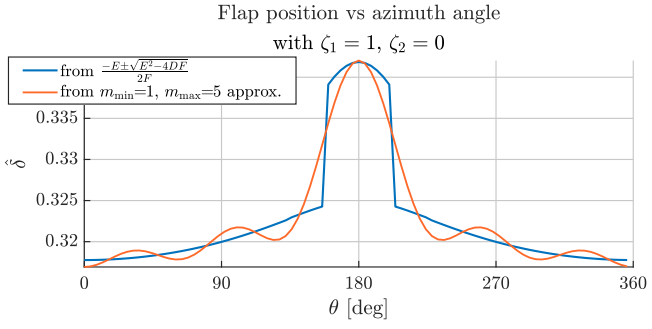


Figure 8. Comparison of flap deflection along the azimuth

These values quantify reductions in the hormonic-load index. They do not establish reductions in structural vibration amplitudes or fatigue damage, which would require coupling to an aeroelastic model. See a discussion on the use of BEM to predict load reduction with flaps in Prospathopoulos et al. (2021).

https://doi.org/10.5194/wes-2026-169
Preprint. Discussion started: 20 November 2026
© Author(s) 2026. CC BY 4.0 License.



WIND ENERGY SCIENCE DISCUSSIONS

3.3 Example 3 - nonlinear coefficients

Consider that the coefficients are now given by the piecewise nonlinear function that follows, with the 15th element plotted in Fig. 9, and the same parameters as before. Using the Theorem for nonlinear coefficients, the results follow

$$C_{(\mathrm{L})i}(\hat{\delta}) = C_{(\mathrm{L})i}(0) +$$
$$S_{(\mathrm{L})i}\hat{\delta}\left(1 - \frac{3}{2}\sin\left(\hat{\delta} - \frac{1}{3}\right)\mathbf{1}_{\hat{\delta}\notin\mathcal{D}}\right) - \frac{1}{2}S_{(\mathrm{L})i}\left(\hat{\delta} - \frac{1}{3}\right)^2\mathbf{1}_{\hat{\delta}\in\mathcal{D}},$$

$$C_{(\mathrm{D})i}(\hat{\delta}) = C_{(\mathrm{D})i}(0) +$$
$$S_{(\mathrm{D})i}\hat{\delta}\left(1 - \frac{3}{2}\sin\left(\hat{\delta} - \frac{1}{3}\right)\mathbf{1}_{\hat{\delta}\notin\mathcal{D}}\right) - \frac{1}{2}S_{(\mathrm{D})i}\left(\hat{\delta} - \frac{1}{3}\right)^2\mathbf{1}_{\hat{\delta}\in\mathcal{D}},$$

$$\mathcal{D} = [0, 0.2] \cup [0.5, 1],$$

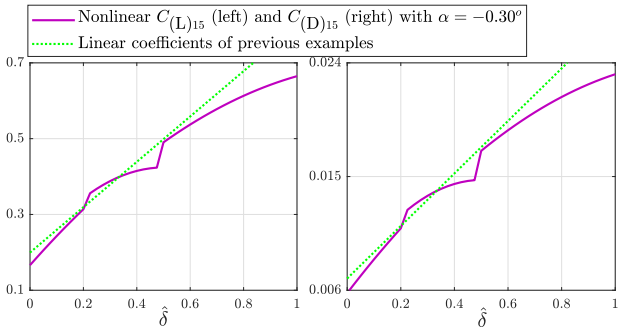


Figure 9. Nonlinear coefficients.

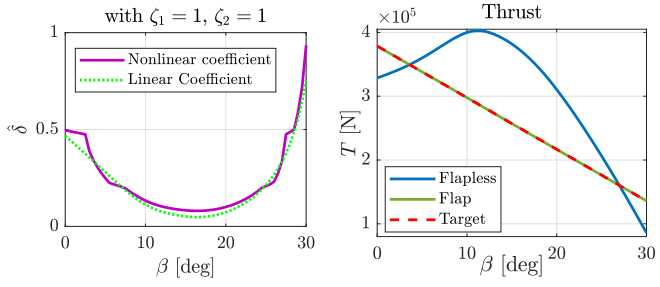


Figure 10. Flap position vs pitch angle (left) and corresponding thrust (right).

In this example, the lift and drag coefficients are described by discountinuous functions. Althought the derivatives in lines 36 and 40 of Algorithm A3 could be approximated by finite differences spanning the discontinuities, such approximations must be interpreted with caution, as the derivatives are undefined at the discontinuity points.

4 Conclusions

The contribution of this paper is a method based on the blade element momentum theory to determine a flap position that minimizes the difference between target and actual aerodynamic loads according to weighting parameters. The method is adequate

https://doi.org/10.5194/wes-2026-169
Preprint. Discussion started: 20 November 2026
© Author(s) 2026. CC BY 4.0 License.



eawe european academy of wind energy
Open Access WIND ENERGY SCIENCE DISCUSSIONS

for single or multiple flaps and affine or nonlinear lift/drag coefficients. All the numerical examples show that prioritized loads are accurately tracked, which means that the method is adequate for applications where a precise flap control is required, such as the root bending moment responsivity compensation, or wind induced load pulsation.

Code and data availability. the Algorithm in Matlab code and numerical examples are available in osf.io/2aczr

Appendix A: Appendix - the algorithm

Inputs Air density ρ; For $i = 1, \cdots, n$: Blade element radii r_i; Chord lengths c_i; Local twists γ_i; Normalized inflow speeds $v_{(\infty)i}$. For $j_V, j_\Omega, j_\beta = 1, ..., N_V, N_\Omega, N_\beta$: Blade pitch angles $\beta_{(\text{grid})j_\beta}$; Inflow multipliers $V_{(\text{grid})j_V}$; Rotor speeds $\Omega_{(\text{grid})j_\Omega}$; Set of angles of attack $X_\alpha = \{\alpha_{(\text{grid})j_\alpha} : j_\alpha = 1, \cdots, N_\alpha\}$.

Either linear coefficients sets:

$X_{C_{(\text{D})i}} = \{C_{(\text{D,grid})i,j_\alpha} : j_\alpha = 1, \cdots, N_\alpha\}$,
$X_{C_{(\text{L})i}} = \{C_{(\text{L,grid})i,j_\alpha} : j_\alpha = 1, \cdots, N_\alpha\}$,
$X_{S_{(\text{D})i}} = \{S_{(\text{D,grid})i,j_\alpha} : j_\alpha = 1, \cdots, N_\alpha\}$,
$X_{S_{(\text{L})i}} = \{S_{(\text{L,grid})i,j_\alpha} : j_\alpha = 1, \cdots, N_\alpha\}$

or set of flap deflections $X_\delta = \{\delta_{(\text{grid})j_\delta} : j_\delta = 1, \cdots, N_\delta\}$ and nonlinear coefficients sets:

$X_{C_{(\text{D})i}} = \{C_{(\text{D,grid})i,j_\alpha,j_\delta} : j_\alpha = 1, \cdots, N_\alpha, j_\delta = 1, \cdots, N_\delta\}$,
$X_{C_{(\text{L})i}} = \{C_{(\text{L,grid})i,j_\alpha,j_\delta} : j_\alpha = 1, \cdots, N_\alpha, j_\delta = 1, \cdots, N_\delta\}$.

Outputs For $i = 1...n$ and $j_V, j_\Omega, j_\beta = 1, ..., N_V, N_\Omega, N_\beta$:

$T_{(\text{grid})i,j_V,j_\Omega,j_\beta}$, $Q_{(\text{grid})i,j_V,j_\Omega,j_\beta}$, $\tau_{(\text{N,grid})i,j_V,j_\Omega,j_\beta}$, $F_{(\text{T,grid})i,j_V,j_\Omega,j_\beta}$ and $\hat{\delta}_{(\text{grid})j_V,j_\Omega,j_\beta}$.

Remarks The equality $j_V, j_\Omega, j_\beta = 1, \cdots, N_V, N_\Omega, N_\beta$ reads as $j_V = 1, \cdots, N_V$ and $j_\Omega = 1, \cdots, N_\Omega$ and $j_\beta = 1, \cdots, N_\beta$; The algorithm uses the equations declared in Section 2.1 with the parameters before Fig. 2, changing $V_{(\infty)i}$ to $V_{(\infty)i} = V v_{(\infty)i}$ where $v_{(\infty)i}$ is the normalized wind profile and V is a multiplier.

The coefficients are interpolated from the look-up tables $C_{(\text{L,grid})}$ and $C_{(\text{D,grid})}$. For $x \in [x_{(\text{grid})j}, x_{(\text{grid})j+1})$ with $j \in \{1, \ldots, N-1\}$, let $\lambda(x) = \dfrac{x - x_{(\text{grid})j}}{x_{(\text{grid})j+1} - x_{(\text{grid})j}} \in [0, 1)$. The one-dimensional interpolation is defined as

$$\mathcal{I}[f, X](x) \triangleq (1 - \lambda(x)) f(x_{(\text{grid})j}) + \lambda(x) f(x_{(\text{grid})j+1})$$

where $X = \{x_{(\text{grid})j} : j \in \{1, \ldots, N\}\}$ is a set with N strictly increasing look-up table grid points, and $f : X \mapsto \mathbb{R}$. In the Matlab code, the function f and set X are directly given as arguments for the `interp1` or `interp2` command.

Finally, $dr_i = \begin{cases} r_2 - r_1, & i = 1, \\ \dfrac{r_{i+1} - r_{i-1}}{2}, & 2 \le i \le n-1, \\ r_n - r_{n-1}, & i = n. \end{cases}$

https://doi.org/10.5194/wes-2026-169
Preprint. Discussion started: 20 November 2026
© Author(s) 2026. CC BY 4.0 License.



eawe european academy of wind energy
Open Access WIND ENERGY SCIENCE DISCUSSIONS

Algorithm A1 Interpolate Coefficients

if coefficients are linear **then**

Define $\begin{cases} f_{C_{(\mathrm{L})i}} : X_\alpha \mapsto X_{C_{(\mathrm{L})i}}, f_{S_{(\mathrm{L})i}} : X_\alpha \mapsto X_{S_{(\mathrm{L})i}}, \\ f_{C_{(\mathrm{D})i}} : X_\alpha \mapsto X_{C_{(\mathrm{D})i}}, f_{S_{(\mathrm{D})i}} : X_\alpha \mapsto X_{S_{(\mathrm{D})i}}. \end{cases}$

$C_{(\mathrm{L})i}(0) \leftarrow \mathcal{I}\left[f_{C_{(\mathrm{L})i}}, X_\alpha\right](\alpha_i)$

$C_{(\mathrm{D})i}(0) \leftarrow \mathcal{I}\left[f_{C_{(\mathrm{D})i}}, X_\alpha\right](\alpha_i)$

$C_{(\mathrm{N})i}(0) \leftarrow C_{(\mathrm{L})i}(0)\cos\phi_i + C_{(\mathrm{D})i}(0)\sin\phi_i$

$C_{(\mathrm{T})i}(0) \leftarrow C_{(\mathrm{L})i}(0)\sin\phi_i - C_{(\mathrm{D})i}(0)\cos\phi_i$

$S_{(\mathrm{L})i} \leftarrow \mathcal{I}\left[f_{S_{(\mathrm{L})i}}, X_\alpha\right](\alpha_i)$

$S_{(\mathrm{D})i} \leftarrow \mathcal{I}\left[f_{S_{(\mathrm{D})i}}, X_\alpha\right](\alpha_i)$

$S_{(\mathrm{N})i} \leftarrow S_{(\mathrm{L})i}\cos\phi_i + S_{(\mathrm{D})i}\sin\phi_i$

$S_{(\mathrm{T})i} \leftarrow S_{(\mathrm{L})i}\sin\phi_i - S_{(\mathrm{D})i}\cos\phi_i$

$C_{(\mathrm{N})i} \leftarrow C_{(\mathrm{N})i}(0) + S_{(\mathrm{N})i}\delta_i$

$C_{(\mathrm{T})i} \leftarrow C_{(\mathrm{T})i}(0) + S_{(\mathrm{T})i}\delta_i$

else

Define $\begin{cases} f_{C_{(\mathrm{L})i}} : X_\alpha \times X_\delta \mapsto X_{C_{(\mathrm{L})i}}, \\ f_{C_{(\mathrm{D})i}} : X_\alpha \times X_\delta \mapsto X_{C_{(\mathrm{D})i}}. \end{cases}$

$C_{(\mathrm{L})i} \leftarrow \mathcal{I}\left[f_{C_{(\mathrm{L})i}}, X_\alpha, X_\delta\right](\alpha_i, \delta_i)$

$C_{(\mathrm{D})i} \leftarrow \mathcal{I}\left[f_{C_{(\mathrm{D})i}}, X_\alpha, X_\delta\right](\alpha_i, \delta_i)$

$C_{(\mathrm{N})i} \leftarrow C_{(\mathrm{L})i}\cos\phi_i + C_{(\mathrm{D})i}\sin\phi_i$

$C_{(\mathrm{T})i} \leftarrow C_{(\mathrm{L})i}\sin\phi_i - C_{(\mathrm{D})i}\cos\phi_i$

end if

https://doi.org/10.5194/wes-2026-169
Preprint. Discussion started: 20 November 2026
© Author(s) 2026. CC BY 4.0 License.



eawe european academy of wind energy
Open Access WIND ENERGY SCIENCE DISCUSSIONS

Algorithm A2 Find $\hat{\delta}$

if $\mathcal{F} = \varnothing$ **then**
  All flaps are in the neutral position.
  $\hat{\delta} \leftarrow \delta_x$
  $\hat{\delta}_{(\text{prev})} \leftarrow \delta_x$
  $d \leftarrow 2$
else if $d \neq 0$ **then**
  $\hat{\delta}_{(\text{prev})} \leftarrow \hat{\delta}$
  if $|F| < \varepsilon$ **then**
    if $E < -\varepsilon$ **then**
      $\hat{\delta} \leftarrow -\dfrac{D}{E}$
    else if $E > \varepsilon$ **then**
      if $2D + E > 0$ **then**
        $\hat{\delta} \leftarrow 1$
      else
        $\hat{\delta} \leftarrow 0$
      end if
    else
      if $D > \varepsilon$ **then**
        $\hat{\delta} \leftarrow 1$
      else if $D < -\varepsilon$ **then**
        $\hat{\delta} \leftarrow 0$
      else
        $\hat{\delta} \leftarrow \hat{\delta}_{(\text{prev})}$
      end if
    end if
  else
    if $E^2 - 4DF \leq 0$ **then**
      if $F > 0$ **then**
        $\hat{\delta} \leftarrow 1$
      else
        $\hat{\delta} \leftarrow 0$
      end if
    else
      $\hat{\delta}_+ \leftarrow \dfrac{-E + \sqrt{E^2 - 4DF}}{2F}$
      $\hat{\delta}_- \leftarrow \dfrac{-E - \sqrt{E^2 - 4DF}}{2F}$
      if $E + 2F\hat{\delta}_+ < 0$ **then**
        $\hat{\delta} \leftarrow \hat{\delta}_+$
      else
        $\hat{\delta} \leftarrow \hat{\delta}_-$
      end if
    end if
  end if
  $\hat{\delta} \leftarrow \min\left(\max(\hat{\delta}, 0), 1\right)$
  Impose the bounds $0 \leq \hat{\delta} \leq 1$.
  if $\left|\hat{\delta} - \hat{\delta}_{(\text{prev})}\right| \leq \varepsilon_\delta$ **then**
    $\hat{\delta} \leftarrow \hat{\delta}_{(\text{prev})}$
    $d \leftarrow 2$
    Terminate the iteration.
  end if
else
  $\hat{\delta}_{(\text{prev})} \leftarrow \delta_x$
  if $\delta_x + \Delta\delta_x \leq 1$ **then**
    $\hat{\delta} \leftarrow \delta_x + \Delta\delta_x$
  else
    $\hat{\delta} \leftarrow \delta_x - \Delta\delta_x$
  end if
  $d \leftarrow 1$
  Perform a second evaluation to compute the first derivatives.
end if

https://doi.org/10.5194/wes-2026-169
Preprint. Discussion started: 20 November 2026
© Author(s) 2026. CC BY 4.0 License.



eawe european academy of wind energy
Open Access WIND ENERGY SCIENCE DISCUSSIONS

Algorithm A3 Main loop

for $j_V = 1, \ldots, N_V$ **do**
  for $j_\Omega = 1, \ldots, N_\Omega$ **do**
    for $j_\beta = 1, \ldots, N_\beta$ **do**
      $d \leftarrow 0$
      while $d \neq 2$ **do**
        $d = 0$*: initial evaluation with* $\delta_i = \delta_x$*;* $d = 1$*: subsequent iterations;* $d = 2$*: termination.*
        for $i = 1, \ldots, n$ **do**
          Evaluate blade element i*.*
          if $i \notin \mathcal{F}$ or $d = 0$ **then**
            The initial flap deflection guess: $\delta_i \leftarrow \delta_x$
          else
            Store previous values: $\delta_{(\text{prev})i} \leftarrow \delta_i$; $q_{(\text{prev})i} \leftarrow q_i$; $C_{(\text{N})(\text{prev})i} \leftarrow C_{(\text{N})i}$; $C_{(\text{T})(\text{prev})i} \leftarrow C_{(\text{T})i}$
            Apply computed flap deflection to stations: $\delta_i \leftarrow \hat{\delta}$
          end if
          $a_i \leftarrow 0.3$, $b_i \leftarrow 0.01$
          Initialize the induction-factor estimates.
          $a_{(\text{tol})i} \leftarrow 0.00001\, a_i$, $b_{(\text{tol})i} \leftarrow 0.00001\, b_i$
          $\Delta a_i \leftarrow |2a_{(\text{tol})i}|$, $\Delta b_i \leftarrow |2b_{(\text{tol})i}|$
          while $\Delta a_i \geq a_{(\text{tol})i}$ or $\Delta b_i \geq b_{(\text{tol})i}$ **do**
            Compute ϕ_i *according to Eq. (1):*
            $$\phi_i \leftarrow \arctan\left(\frac{(1-a_i)V_{(\text{grid})j_V}\, v_{(\infty)i}}{(1+b_i)\Omega_{(\text{grid})j_\Omega}\, r_i}\right)$$
            Compute α_i *according to Eq. (4):*
            $$\alpha_i \leftarrow \phi_i - \left(\beta_{(\text{grid})j_\beta} + \gamma_i\right)$$
            Call Algorithm A1 to interpolate coefficents.
            Update a_i *according to Eq. (5):*
            $$a_{(\text{new})i} \leftarrow \left(1 + \frac{4\sin^2\phi_i}{\sigma_i C_{(\text{N})i}}\right)^{-1}$$
            Update b_i *according to Eq. (6):*
            $$b_{(\text{new})i} \leftarrow \left(\frac{4\sin\phi_i\cos\phi_i}{\sigma_i C_{(\text{T})i}} - 1\right)^{-1}$$
            $\Delta a_i \leftarrow |a_{(\text{new})i} - a_i|$
            $\Delta b_i \leftarrow |b_{(\text{new})i} - b_i|$
            $a_i \leftarrow 0.75a_i + 0.25a_{(\text{new})i}$
            $b_i \leftarrow 0.75b_i + 0.25b_{(\text{new})i}$
          end while
          Compute $V_{(\text{rel})i}$ *according to Eq. (2):*
          $$V_{(\text{rel})i} \leftarrow \sqrt{\left[V_{(\text{grid})j_V}\, v_{(\infty)i}(1-a_i)\right]^2 + \left[\Omega_{(\text{grid})j_\Omega}(1+b_i)r_i\right]^2}$$
          Compute q_i *according to Eq. (3):*
          $$q_i \leftarrow \frac{1}{2}\rho V_{(\text{rel})i}^2\, c_i\, dr_i$$
          Compute loads:
          $T_{(\text{grid})i,j_V,j_\Omega,j_\beta} \leftarrow q_i C_{(\text{N})i}$
          $F_{(\text{T,grid})i,j_V,j_\Omega,j_\beta} \leftarrow q_i C_{(\text{T})i}$
          $\tau_{(\text{N,grid})i,j_V,j_\Omega,j_\beta} \leftarrow T_{(\text{T,grid})i,j_V,j_\Omega,j_\beta}\, r_i$
          $Q_{(\text{grid})i,j_V,j_\Omega,j_\beta} \leftarrow F_{(\text{T,grid})i,j_V,j_\Omega,j_\beta}\, r_i$
          if $d \neq 0$ and $i \in \mathcal{F}$ **then**
            After the initial evaluation, compute derivatives only at the flap stations
            $$\frac{dq_i}{d\delta} \leftarrow \frac{q_i - q_{(\text{prev})i}}{\delta_i - \delta_{(\text{prev})i}}$$
            if coefficients are linear **then**
              Build D, E, and F as in the corollary.
            else
              Compute the normal and tangential coefficient derivatives:
              $$\frac{dC_{(\text{N})i}}{d\delta} \leftarrow \frac{C_{(\text{N})i} - C_{(\text{N})(\text{prev})i}}{\delta_i - \delta_{(\text{prev})i}}$$
              $$\frac{dC_{(\text{T})i}}{d\delta} \leftarrow \frac{C_{(\text{T})i} - C_{(\text{T})(\text{prev})i}}{\delta_i - \delta_{(\text{prev})i}}$$
              Build D, E, and F as in the theorem.
            end if
          end if
        end for
        Call Algorithm A2 to find $\hat{\delta}$.
      end while
      $\hat{\delta}_{(\text{grid})j_V,j_\Omega,j_\beta} \leftarrow \hat{\delta}$
    end for
  end for
end for

https://doi.org/10.5194/wes-2026-169
Preprint. Discussion started: 20 November 2026
© Author(s) 2026. CC BY 4.0 License.



eawe european academy of wind energy
Open Access WIND ENERGY SCIENCE DISCUSSIONS

Author contributions. Arthur Scolari Fagundes: Conceptualization and article writing

Competing interests. No competing interests are present

Acknowledgements. This work was supported by the PHC Ulysses programme (Project No. 51961NP), funded by the French Ministry for Europe and Foreign Affairs, the French Ministry for Higher Education and Research, Taighde Éireann – Research Ireland, RTE France, EirGrid, ADEME, and SEAI. From the Irish side, the relevant award is Taighde Éireann – Research Ireland / Ulysses (Grant No. RI/IRC/Ulysses/2025/41_NEPOMUC).

https://doi.org/10.5194/wes-2026-169
Preprint. Discussion started: 20 November 2026
© Author(s) 2026. CC BY 4.0 License.



eawe european academy of wind energy
Open Access WIND ENERGY SCIENCE DISCUSSIONS

References

Barlas, T. K. and van Kuik, G. A. M.: Review of state of the art in smart rotor control research for wind turbines, Progress in Aerospace Sciences, 46, 1–27, https://doi.org/10.1016/j.paerosci.2009.08.002, 2010.

Bossanyi, E. A.: Individual Blade Pitch Control for Load Reduction, Wind Energy, 6, 119–128, https://doi.org/10.1002/we.76, 2003.

Branlard, E.: Wind Turbine Aerodynamics and Vorticity-Based Methods: Fundamentals and Recent Applications, chap. The Blade Element Momentum (BEM) Method, pp. 181–211, Springer International Publishing, Cham, https://doi.org/10.1007/978-3-319-55164-7_10, 2017.

Friedmann, P. P. and Millott, T. A.: Vibration Reduction in Rotorcraft Using Active Control: A Comparison of Various Approaches, Journal of Guidance, Control, and Dynamics, 18, 664–673, https://doi.org/10.2514/3.21445, 1995.

Gamberini, A., Barlas, T., Gomez Gonzalez, A., and Madsen, H. A.: Validation of aeroelastic dynamic model of active trailing edge flap system tested on a 4.3 MW wind turbine, Wind Energy Science, 9, 1229–1249, https://doi.org/10.5194/wes-9-1229-2024, 2024.

Gomez Gonzalez, A., Enevoldsen, P. B., Barlas, A., and Madsen, H. A.: Field test of an active flap system on a full-scale wind turbine, Wind Energy Science, 6, 33–43, https://doi.org/10.5194/wes-6-33-2021, 2021.

Huang, X., Alavi Moghadam, S. M., Meysonnat, P., Meinke, M., and Schröder, W.: Numerical analysis of the effect of flaps on the tip vortex of a wind turbine blade, International Journal of Heat and Fluid Flow, 77, 336–351, https://doi.org/10.1016/j.ijheatfluidflow.2019.05.004, 2019.

Jelavic, M., Petrovic, V., and Peric, N.: Individual pitch control of wind turbine based on loads estimation, in: 2008 34th Annual Conference of IEEE Industrial Electronics, pp. 228–234, https://doi.org/10.1109/IECON.2008.4757957, 2008.

Leishman, J. G. and Johnson, B.: Engineering Analysis of the 1907 Cornu Helicopter, Journal of the American Helicopter Society, 54, 034 001, https://doi.org/10.4050/JAHS.54.034001, 2009.

Madsen, H. A.: Wind turbine flap technology development – from laboratory to full scale testing, available in: https://www.nlr.gov/docs/libraries/wind-docs/2-helge-aagaard-madsen-system-eng-flap-dtu-hama-final-v1.pdf?sfvrsn=cc216055_0. Access date: 23/09/2025, 2024.

McWilliam, M., Barlas, T., Madsen, H., and Zahle, F.: Aero-elastic wind turbine design with active flaps for AEP maximization, Wind Energy Science, 3, 231–241, https://doi.org/10.5194/wes-3-231-2018, 2018.

Millott, T. A. and Friedmann, P. P.: Vibration Reduction in Helicopter Rotors Using an Actively Controlled Partial Span Trailing Edge Flap Located on the Blade, Tech. Rep. NASA Contractor Report 4611, National Aeronautics and Space Administration (NASA), 1994.

Prospathopoulos, J. M., Riziotis, V. A., Schwarz, E., Barlas, T., Aparicio-Sanchez, M., Papadakis, G., Manolas, D., Pirrung, G., and Lutz, T.: Simulation of oscillating trailing edge flaps on wind turbine blades using ranging fidelity tools, Wind Energy, 24, 357–378, https://doi.org/10.1002/we.2578, 2021.

Viswamurthy, S. R. and Ganguli, R.: An optimization approach to vibration reduction in helicopter rotors with multiple active trailing edge flaps, Aerospace Science and Technology, 8, 185–194, https://doi.org/10.1016/j.ast.2003.10.003, 2004.